Supporting Information (SI):

Heterogeneous Ni_3P/Ni nanoparticles with optimized Ni active sites anchored in N-doped mesoporous nanofibers for boosting pH-universal hydrogen evolution

Changle Fu[a], Liangliang Feng[a,*], Hongyan Yin[a], Yuhang Li[a], Yajie Xie[a], Yongqiang Feng[a], Yajuan Zhao[a], Liyun Cao[a], Jianfeng Huang[a], Yipu Liu[b,*]

[a] *School of Materials Science & Engineering, Key Laboratory of Auxiliary Chemistry and Technology for Chemical Industry, Ministry of Education, Shaanxi University of Science & Technology, Xi'an Shaanxi, 710021, P.R. China.*

[b] *State Key Laboratory of Marine Resource Utilization in South China Sea, School of Materials Science and Engineering, Hainan University, Haikou 570228 P. R. China*

[*] Corresponding authors.

E-mail addresses: fengll@sust.edu.cn (L. Feng), lyp1992lyp@163.com (Y. Liu).

Number of pages: 42

Number of figures: 30

Number of tables: 8

Containing 42 pages, 30 Figures and 8 Tables

Additional images and data:

Fig. S1. (a) XRD patterns and (b) zoomed-in local patterns of Ni_3P/Ni@N-CNFs-600, Ni_3P/Ni@N-CNFs-700, Ni_3P/Ni@N-CNFs-800 and Ni_3P/Ni@N-CNFs-900.

Fig. S2. SEM images at different magnifications for (a, b) Ni_3P/Ni@N-CNFs-600; (c, d) Ni_3P/Ni@N-CNFs-700; (e, f) Ni_3P/Ni@N-CNFs-800; and (g, h) Ni_3P/Ni@N-CNFs-900.

Fig. S3. (a) SEM image and (b) TEM image of Ni@N-CNFs.

Fig. S4. (a, b) SEM image at different magnifications for Ni_3P.

Fig. S5. The XPS survey spectrum of the Ni_3P/Ni@N-CNFs.

Fig. S6. The N 1s high-resolution XPS spectra of Ni_3P/Ni@N-CNFs-600, Ni_3P/Ni@N-CNFs-800 and Ni_3P/Ni@N-CNFs-900.

Fig. S7. The LSV performance curves of Ni_3P/Ni@N-CNFs-600, Ni_3P/Ni@N-CNFs-700, Ni_3P/Ni@N-CNFs-800 and Ni_3P/Ni@N-CNFs-900 under the condition of 1 M KOH; and (b) the corresponding curve for the relationship between calcination temperature and catalytic performance.

Fig. S8. The XPS survey spectrum of the Ni@N-CNFs and Ni_3P.

Fig. S9. Cyclic voltammetry curves of the samples with different scanning rates (20, 40, 60, 80, 100, 120, 140 mV s^{-1}) for HER in 0.5 M H_2SO_4 electrolyte. (a) Ni_3P/Ni@N-CNFs; (b) Ni@N-CNFs; and (c) Ni_3P.

Fig. S10. LSVs normalized by ECSA of HER under acidic condition.

Fig. S11. The fitted equivalent circuit model of as-synthesized electrocatalysts.

Fig. S12. The Bode plot of Ni_3P/Ni@N-CNFs, Ni@N-CNFs and Ni_3P drawn from EIS measurements.

Fig. S13. (a) The testing device of Faraday efficiency and (b) Hydrogen production efficiency of Ni_3P/Ni@N-CNFs under acidic condition.

Fig. S14. (a) TEM image and (b) HRTEM image of the Ni_3P/Ni@N-CNFs after stability test of *i-t* curve for 60 h at pH 0.

Fig. S15. XPS spectra of the Ni_3P/Ni@N-CNFs after HER electrochemical test in 0.5 M H_2SO_4: (a) C 1s; (b) N 1s; (c) Ni 2p; (d) P 2p.

Fig. S16. The corresponding Tafel slopes the Ni_3P/Ni@N-CNFs and control samples in 1 M KOH.

Fig. S17. Cyclic voltammetry curves of the samples with different scanning rates (10, 20, 40, 60, 80, 100, 120, 140 mV s^{-1}) for HER in 1 M KOH electrolyte. (a) Ni_3P/Ni@N-CNFs; (b) Ni@N-CNFs; and (c) Ni_3P.

Fig. S18. LSVs normalized by ECSA of HER under alkaline condition.

Fig. S19. (a) The double-layer capacitance (C_{dl}) for the evaluation of ECSA and (b) Bode plot of Ni_3P/Ni@N-CNFs, Ni@N-CNFs and Ni_3P in alkaline media.

Fig. S20. (a) TEM image and (b) HRTEM image of the Ni_3P/Ni@N-CNFs after stability test of *i-t* curve for 60 h at pH 14.

Fig. S21. XPS spectra of the Ni_3P/Ni@N-CNFs after HER electrochemical test in 1 M KOH: (a) C 1s; (b) N 1s; (c) Ni 2p; (d) P 2p.

Fig. S22. (a) Multi-step chronoamperometric curve at diverse overpotentials and (b) hydrogen production efficiency of Ni_3P/Ni@N-CNFs under alkaline condition.

Fig. S23. The corresponding Tafel slopes the Ni_3P/Ni@N-CNFs and control samples in 1 M PBS.

Fig. S24. Cyclic voltammetry curves of the samples with different scanning rates (10, 20, 40, 60, 80, 100, 120, 140 mV s^{-1}) for HER in 1 M PBS electrolyte. (a) Ni_3P/Ni@N-CNFs; (b) Ni@N-CNFs; and (c) Ni_3P.

Fig. S25. LSVs normalized by ECSA of HER under neutral condition.

Fig. S26. (a) The double-layer capacitance (C_{dl}) for the evaluation of ECSA and (b) Bode plot of Ni_3P/Ni@N-CNFs, Ni@N-CNFs and Ni_3P in neutral media.

Fig. S27. Multi-step chronoamperometric curve at diverse overpotentials of Ni_3P/Ni@N-CNFs under neutral condition.

Fig. S28. (a) TEM image and (b) HRTEM image of the Ni_3P/Ni@N-CNFs after stability test of *i-t* curve for 60 h at pH 7.

Fig. S29. XPS spectra of the Ni_3P/Ni@N-CNFs after HER electrochemical test in 1 M PBS: (a) C 1s; (b) N 1s; (c) Ni 2p; (d) P 2p.

Fig. S30. Hydrogen production efficiency of Ni_3P/Ni@N-CNFs under neutral condition.

Table S1. Surface elements contents of samples at different temperatures obtained by XPS.

Table S2. (a) The details for calculated fractions of each nitrogen species in the N 1s XPS

spectrum. (b) The details of the proportion of each N species in the whole sample were derived from the calculations.

Table S3. Fitted data from Nyquist plots of as-prepared samples in electrocatalytic HER test under 0.5 M H_2SO_4.

Table S4. Comparison of HER performance between the results from the present research with other recently-reported metal phosphides in 0.5 M H_2SO_4.

Table S5. Fitted data from Nyquist plots of as-prepared samples in electrocatalytic HER test under 1 M KOH.

Table S6. Fitted data from Nyquist plots of as-prepared samples in electrocatalytic HER test under 1 M PBS.

Table S7. Comparison of HER performance between the results from the present research with other recently-reported metal phosphides in 1 M KOH.

Table S8. Comparison of HER performance between the results from the present research with other recently-reported metal phosphides in 1 M PBS.

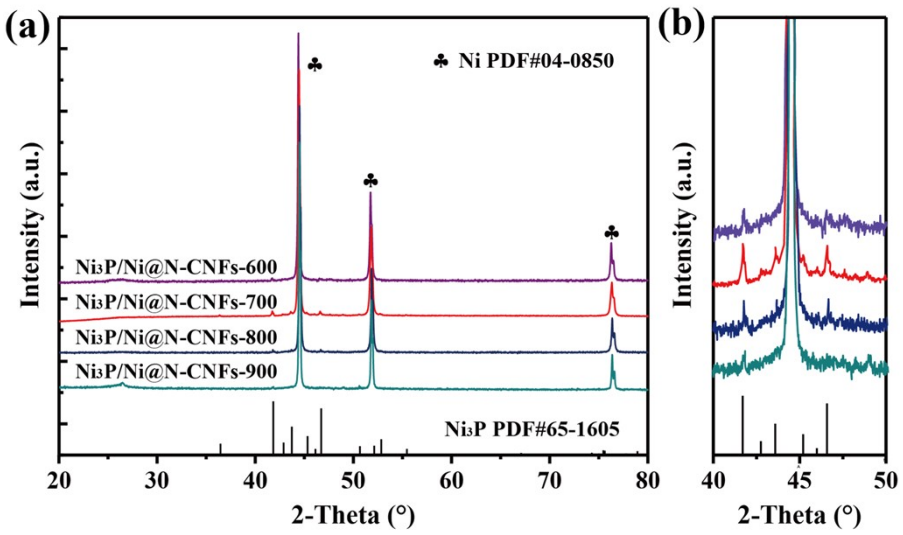

Fig. S1. (a) XRD patterns and (b) zoomed-in local patterns of Ni_3P/Ni@N-CNFs-600, Ni_3P/Ni@N-CNFs-700, Ni_3P/Ni@N-CNFs-800 and Ni_3P/Ni@N-CNFs-900.

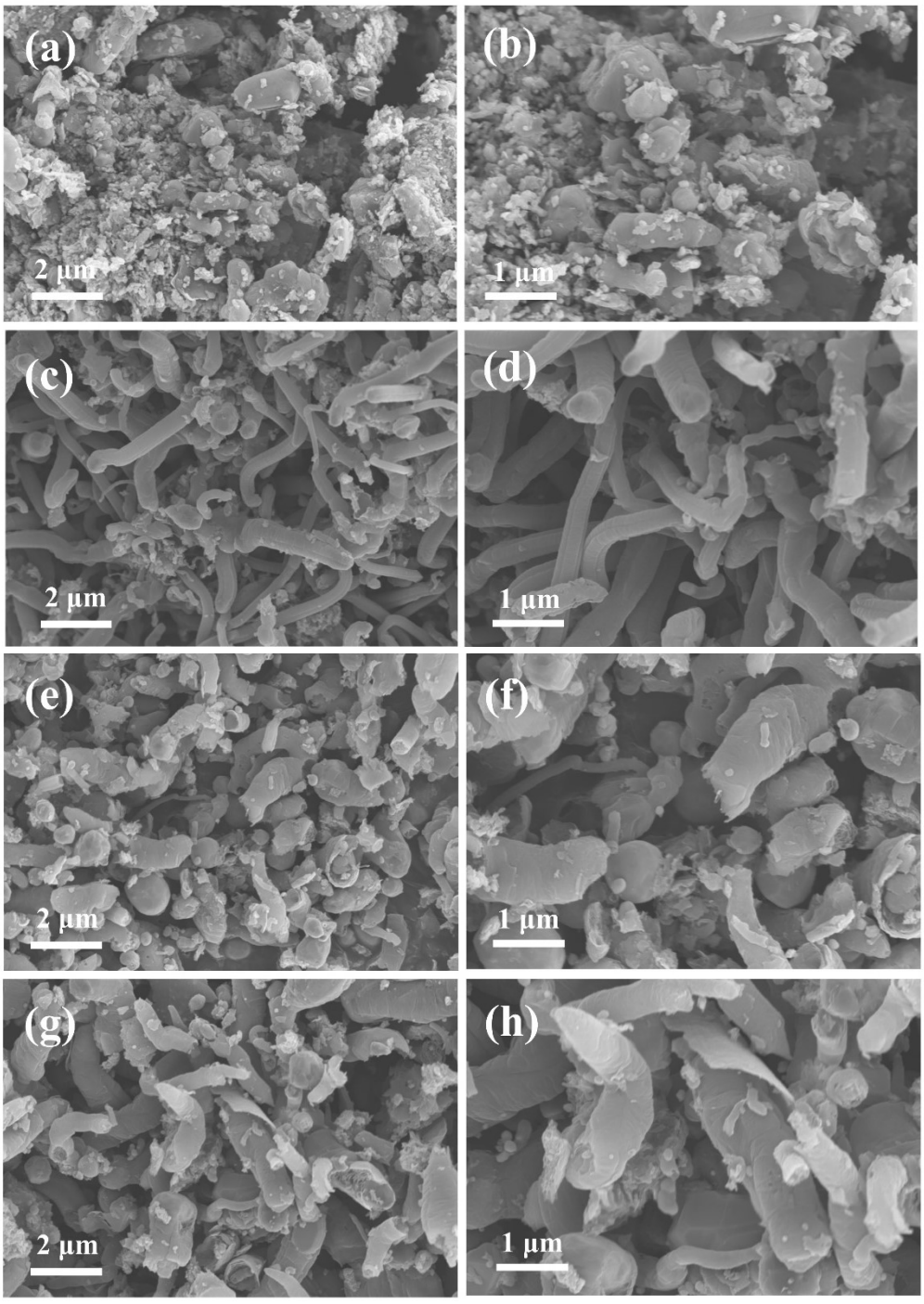

Fig. S2. SEM images at different magnifications for (a, b) Ni_3P/Ni@N-CNFs-600; (c, d) Ni_3P/Ni@N-CNFs-700; (e, f) Ni_3P/Ni@N-CNFs-800; and (g, h) Ni_3P/Ni@N-CNFs-900.

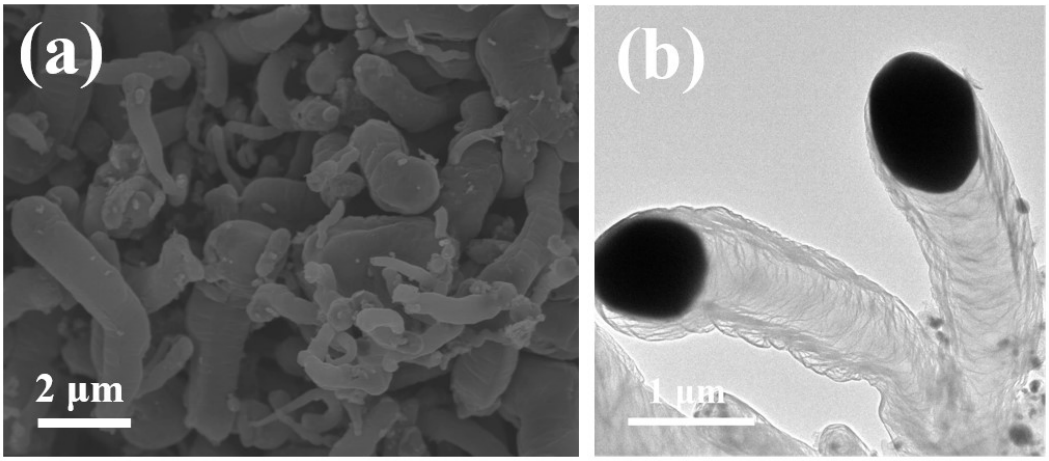

Fig. S3. (a) SEM image and (b) TEM image of Ni@N-CNFs.

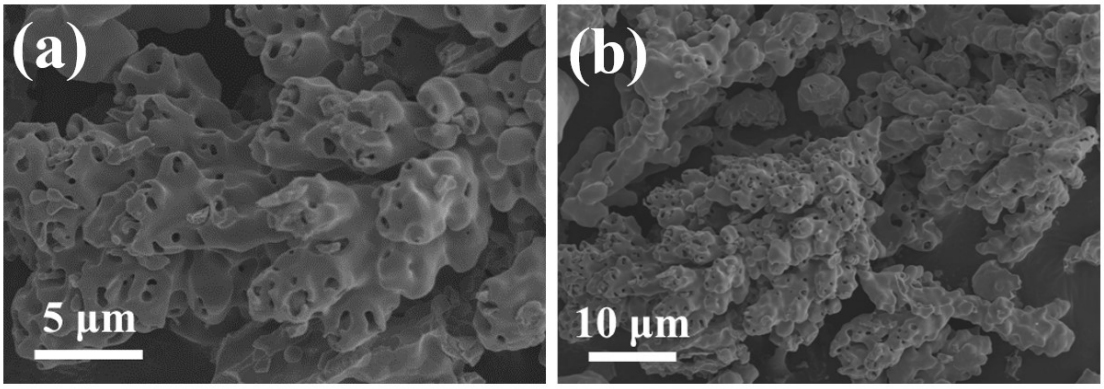

Fig. S4. (a, b) SEM image at different magnifications for Ni_3P.

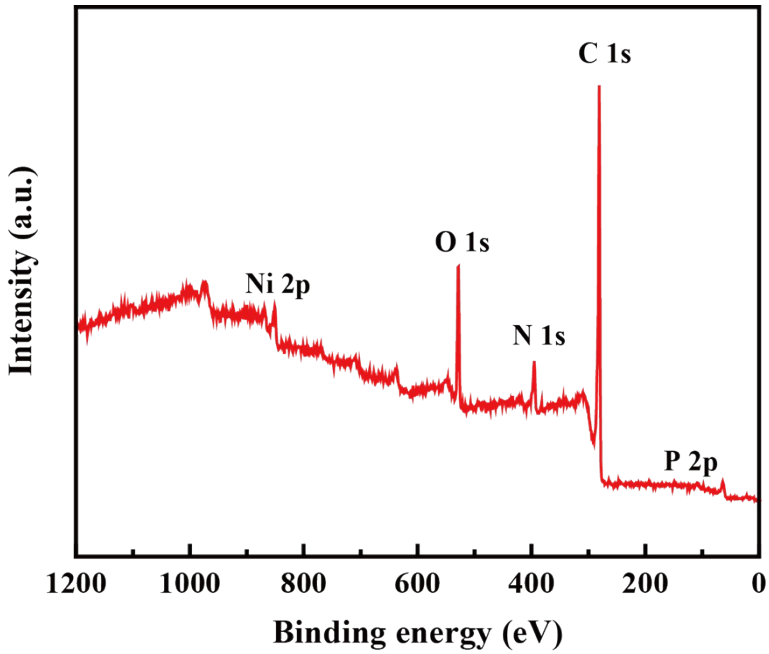

Fig. S5. The XPS survey spectrum of Ni_3P/Ni@N-CNFs.

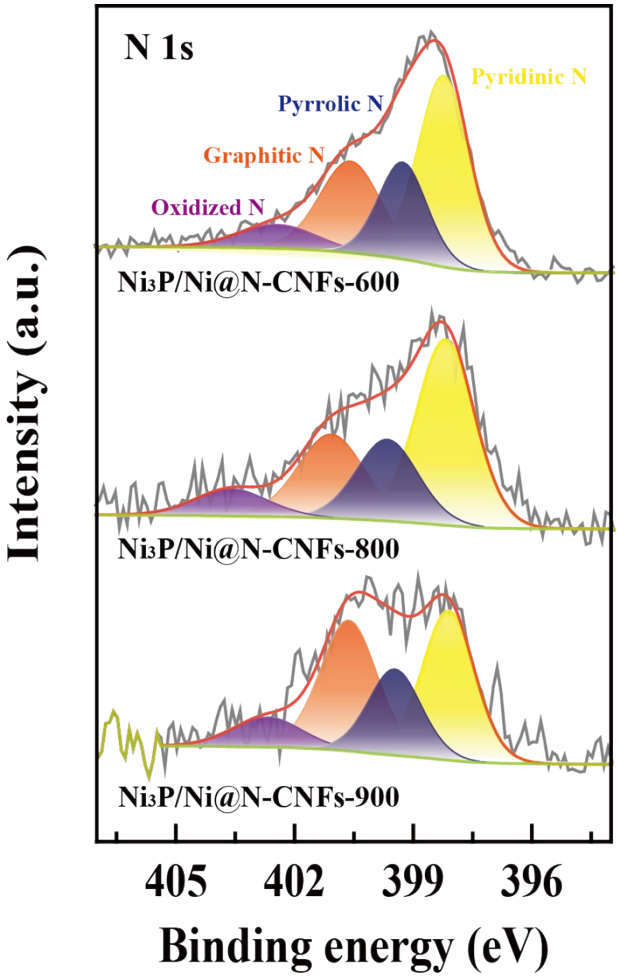

Fig. S6. The N 1s high-resolution XPS spectra of Ni_3P/Ni@N-CNFs-600, Ni_3P/Ni@N-CNFs-800 and Ni_3P/Ni@N-CNFs-900.

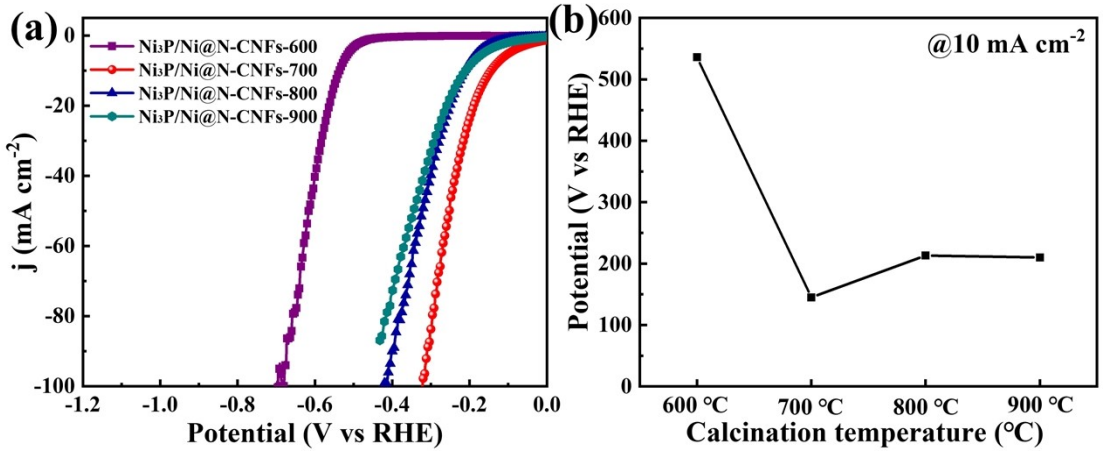

Fig. S7. (a) LSV curves of Ni_3P/Ni@N-CNFs-600, Ni_3P/Ni@N-CNFs-700, Ni_3P/Ni@N-CNFs-800 and Ni_3P/Ni@N-CNFs-900 in 1 M KOH; and (b) the corresponding curve for the relationship between calcination temperature and catalytic performance.

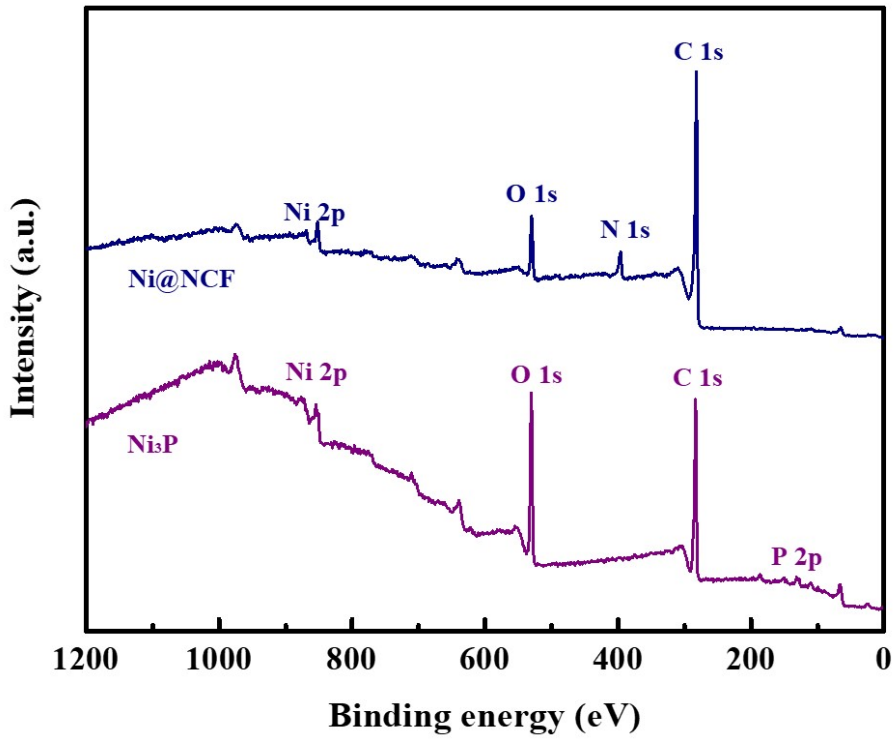

Fig. S8. The XPS survey spectra of the Ni@N-CNFs and Ni_3P.

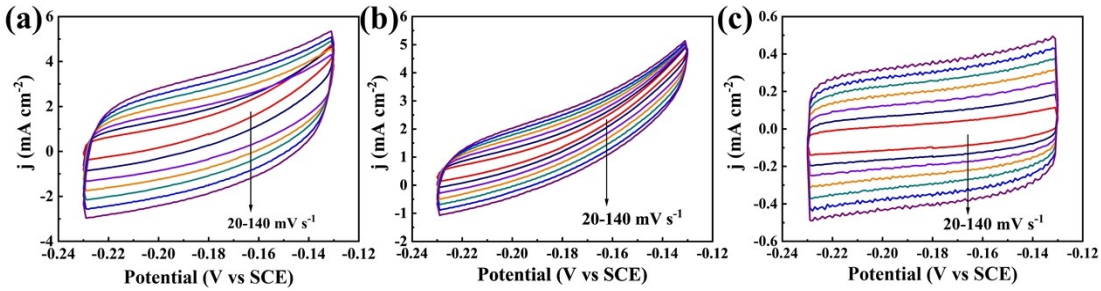

Fig. S9. Cyclic voltammetry curves of the samples with different scanning rates (20, 40, 60, 80, 100, 120, 140 mV s^{-1}) for HER in 0.5 M H_2SO_4 electrolyte. (a) Ni_3P/Ni@N-CNFs; (b) Ni@N-CNFs; and (c) Ni_3P.

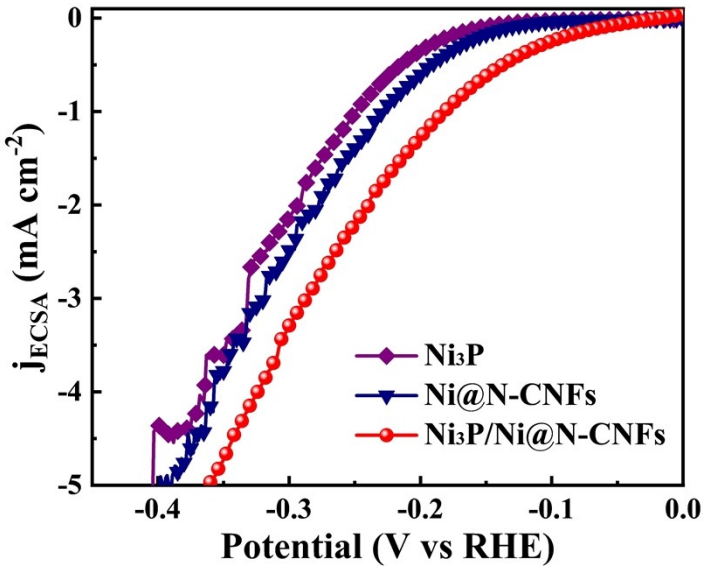

Fig. S10. LSVs normalized by ECSA of HER under acidic condition.

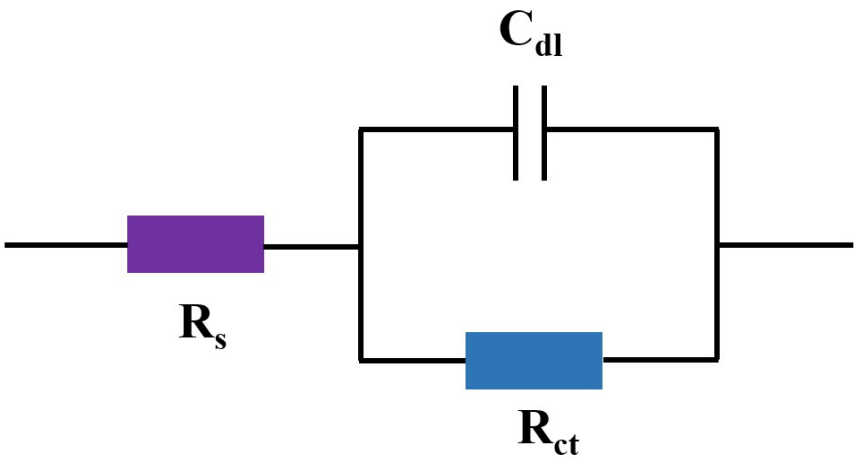

Fig. S11. The fitted equivalent circuit model of as-synthesized electrocatalysts.

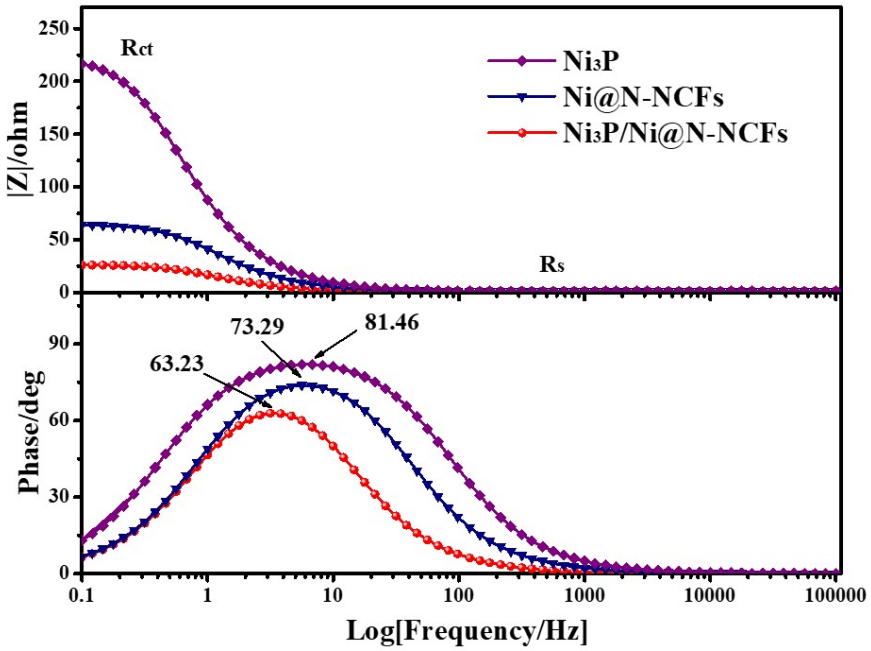

Fig. S12. The Bode plot of Ni_3P/Ni@N-CNFs, Ni@N-CNFs and Ni_3P drawn from EIS measurements.

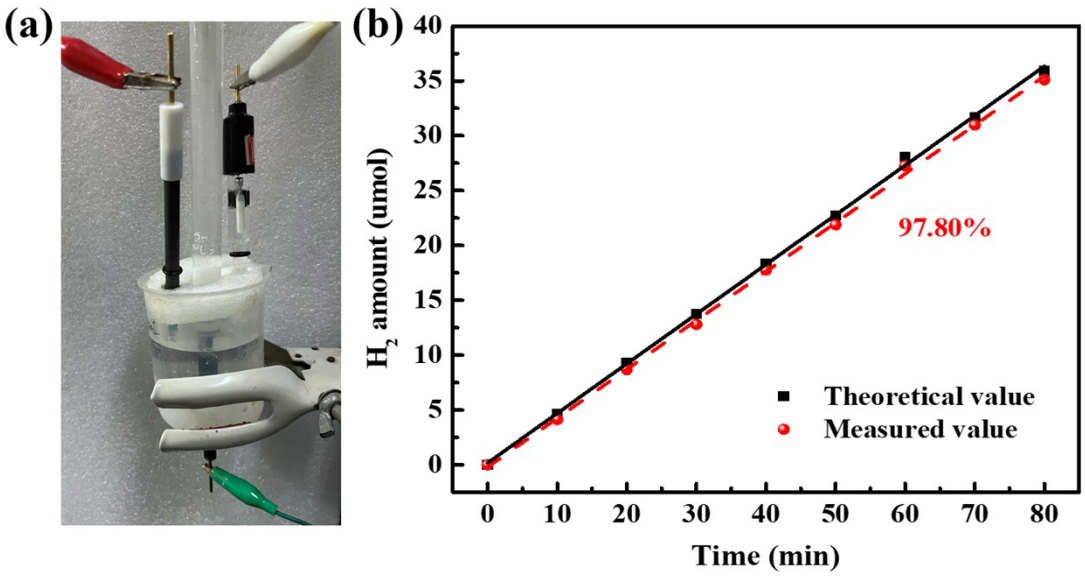

Fig. S13. (a) The testing device of Faraday efficiency and (b) hydrogen production efficiency of Ni_3P/Ni@N-CNFs under the acidic conditions.

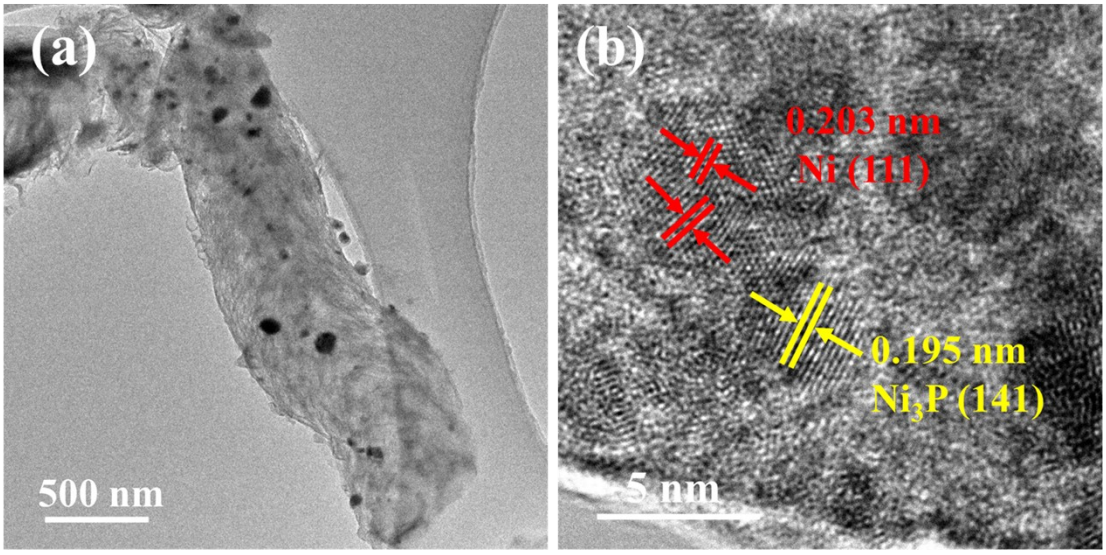

Fig. S14. (a) TEM image and (b) HRTEM image of the Ni_3P/Ni@N-CNFs after stability test of *i-t* curve for 60 h at pH 0.

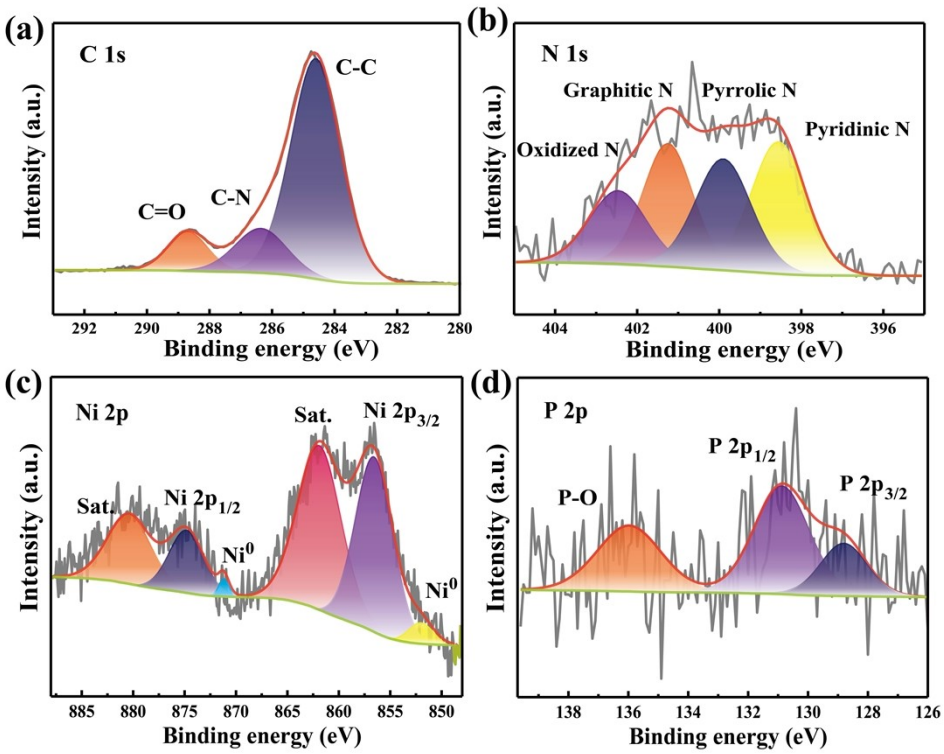

Fig. S15. XPS spectra of the Ni_3P/Ni@N-CNFs after HER electrochemical test in 0.5 M H_2SO_4: (a) C 1s; (b) N 1s; (c) Ni 2p; (d) P 2p.

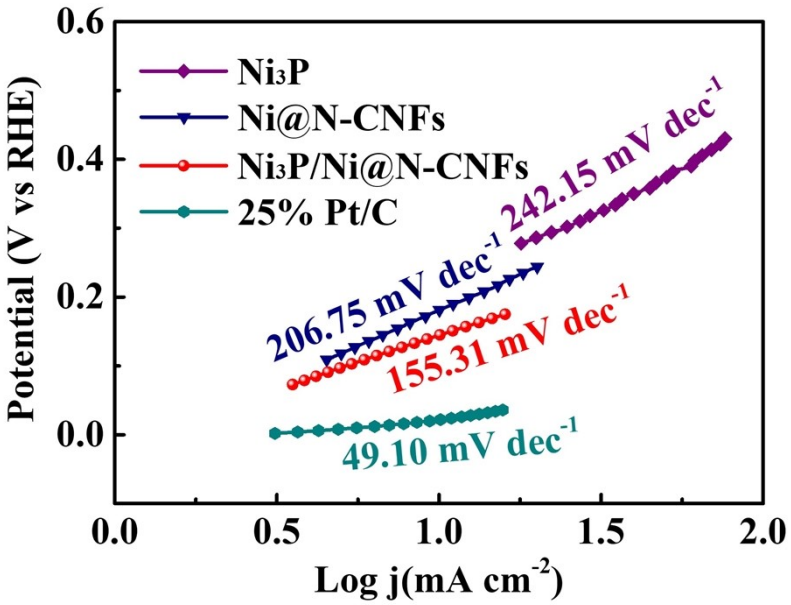

Fig. S16. The corresponding Tafel slopes the Ni_3P/Ni@N-CNFs and control samples in 1 M KOH.

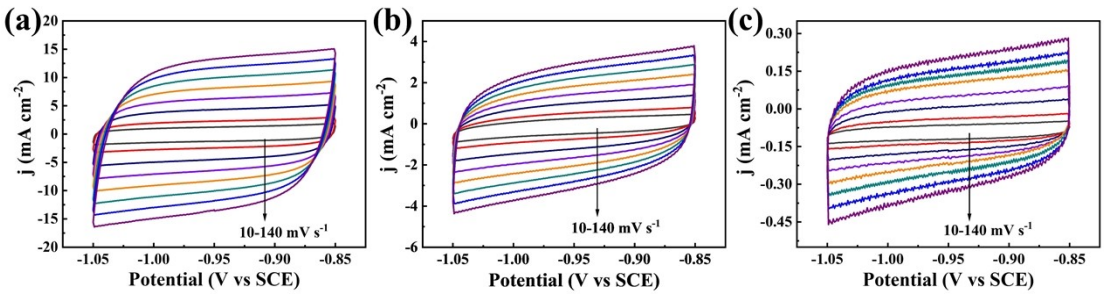

Fig. S17. Cyclic voltammetry curves of the samples with different scanning rates (10, 20, 40, 60, 80, 100, 120, 140 mV s^{-1}) for HER in 1 M KOH electrolyte. (a) Ni_3P/Ni@N-CNFs; (b) Ni@N-CNFs; and (c) Ni_3P.

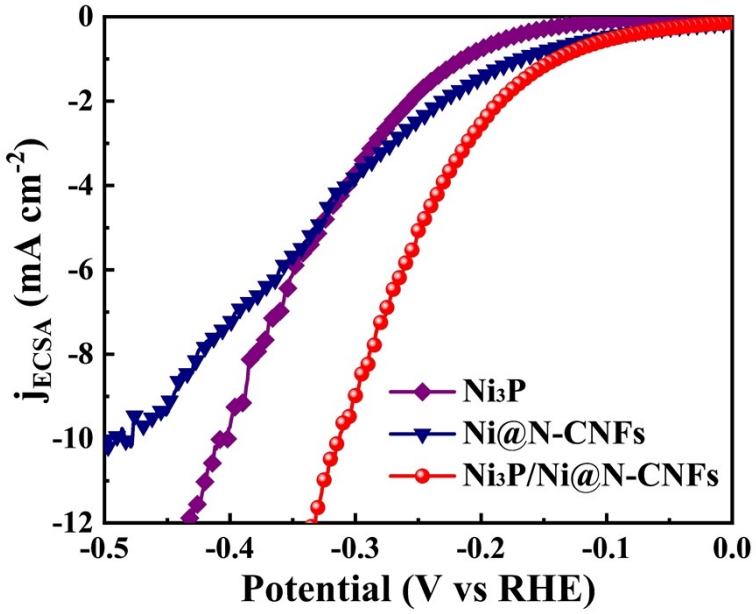

Fig. S18. LSVs normalized by ECSA of HER under alkaline condition.

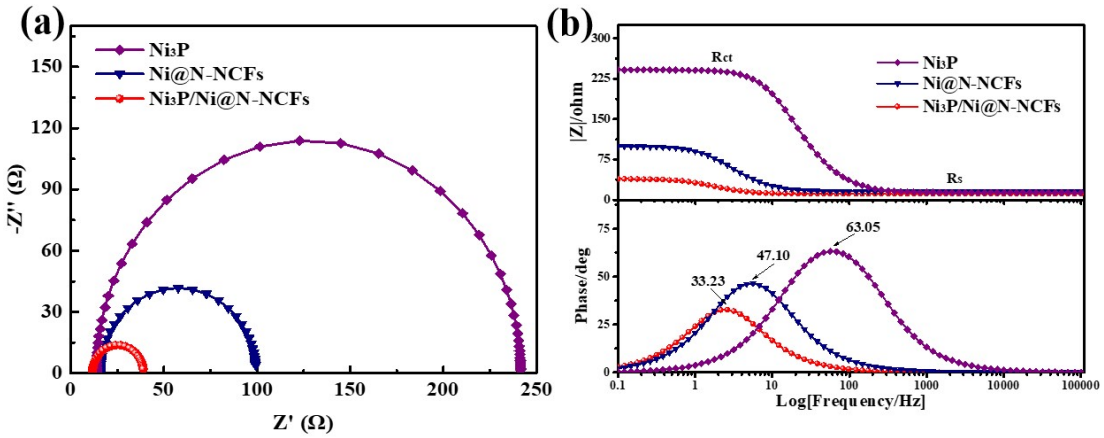

Fig. S19. (a) The double-layer capacitance (C_{dl}) for the evaluation of ECSA and (b) Bode plot of Ni_3P/Ni@N-CNFs, Ni@N-CNFs and Ni_3P in alkaline media.

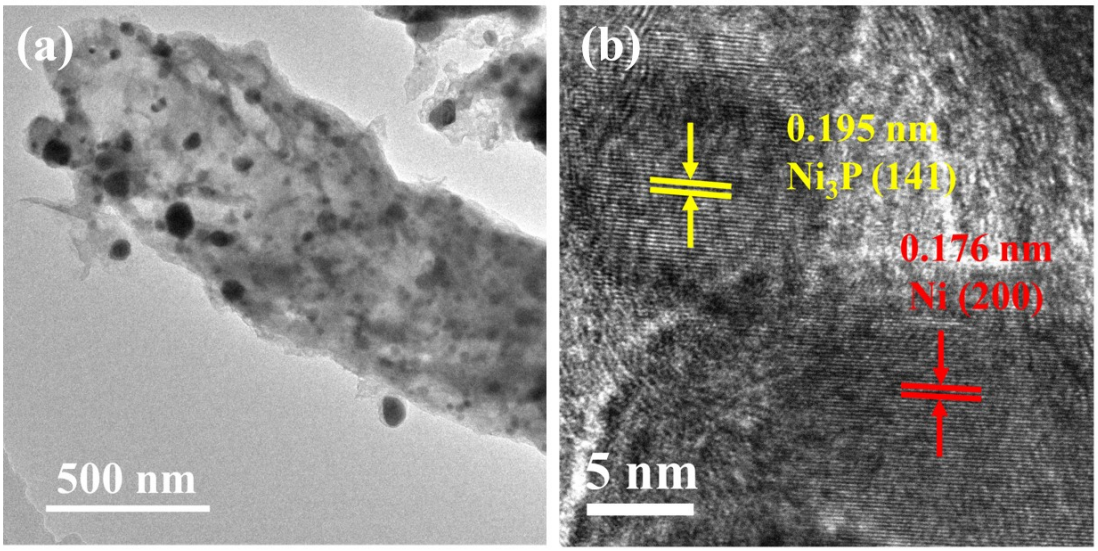

Fig. S20. (a) TEM image and (b) HRTEM image of the Ni_3P/Ni@N-CNFs after stability test of *i-t* curve for 60 h at pH 14.

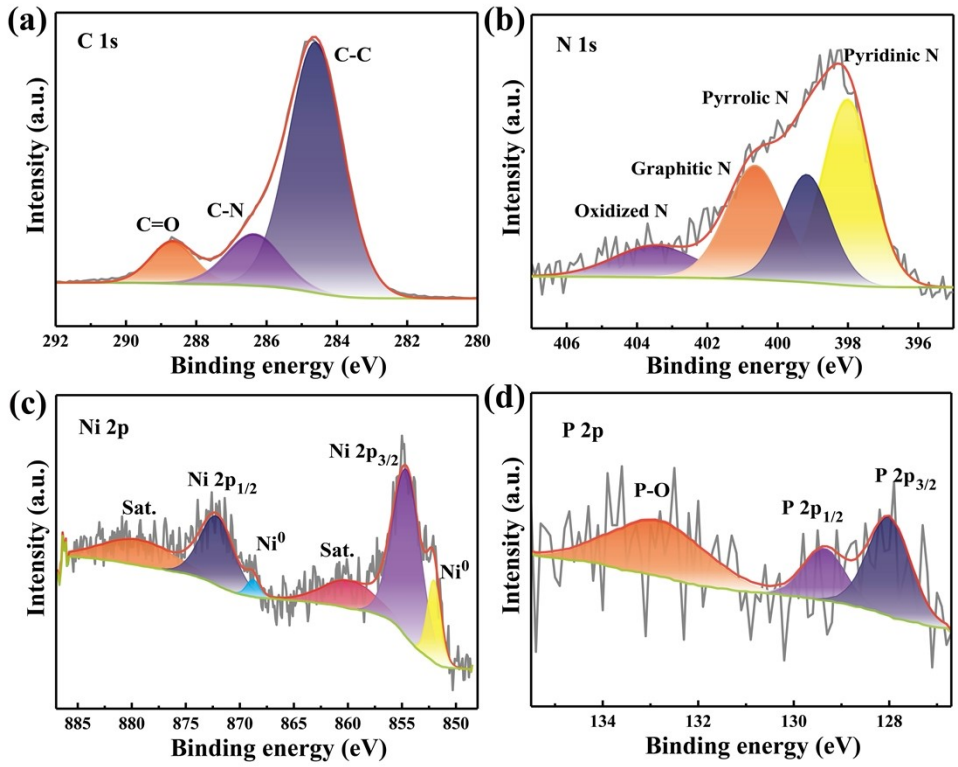

Fig. S21. XPS spectra of the Ni_3P/Ni@N-CNFs after HER electrochemical test in 1 M KOH: (a) C 1s; (b) N 1s; (c) Ni 2p; (d) P 2p.

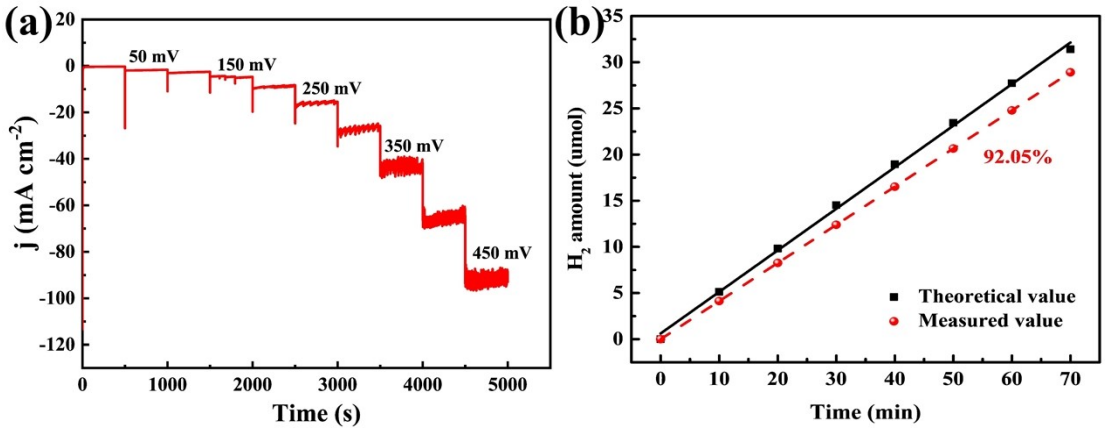

Fig. S22. (a) Multi-step chronoamperometric curve at diverse overpotentials and (b) hydrogen production efficiency of Ni_3P/Ni@N-CNFs under alkaline conditions.

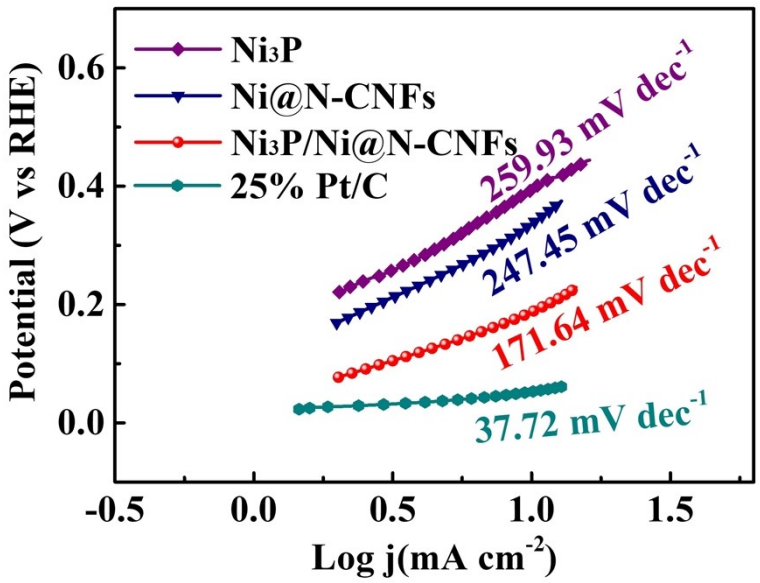

Fig. S23. The corresponding Tafel slopes the Ni_3P/Ni@N-CNFs and control samples in 1 M PBS.

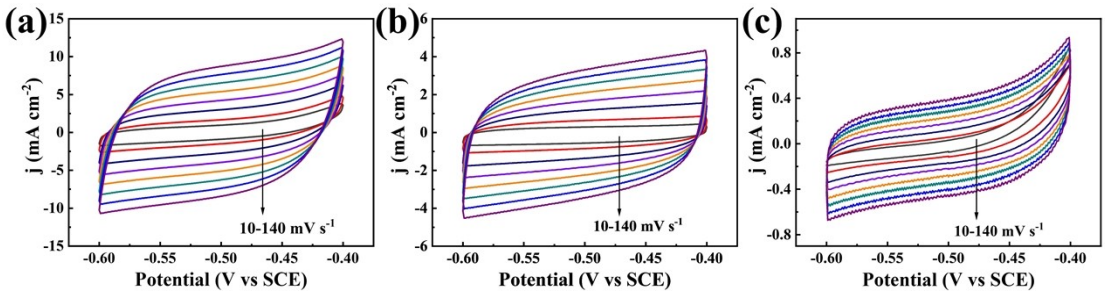

Fig. S24. Cyclic voltammetry curves of the samples with different scanning rates (10, 20, 40, 60, 80, 100, 120, 140 mV s^{-1}) for HER in 1 M PBS electrolyte. (a) Ni_3P/Ni@N-CNFs; (b) Ni@N-CNFs; and (c) Ni_3P.

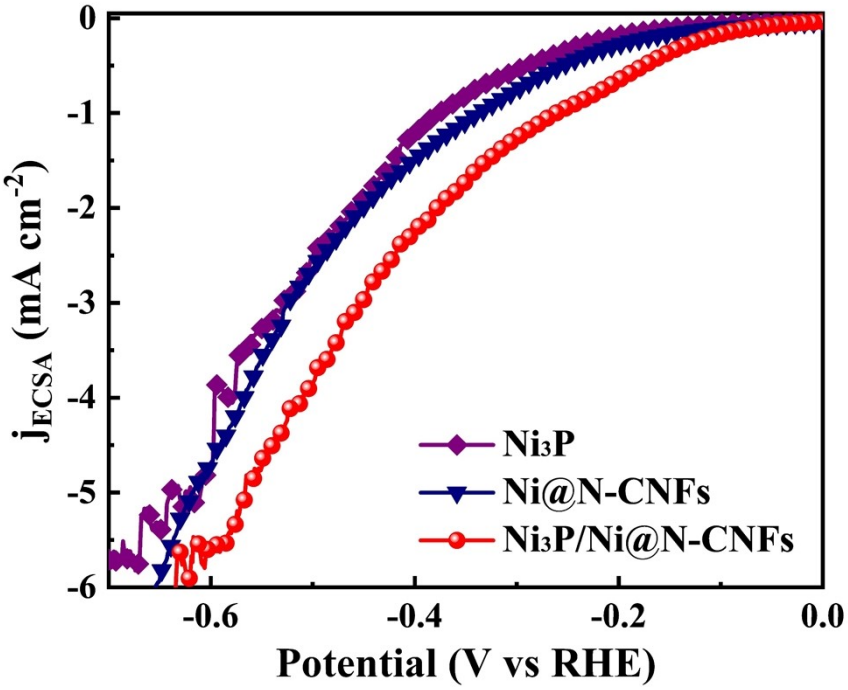

Fig. S25. LSVs normalized by ECSA of HER under neutral condition.

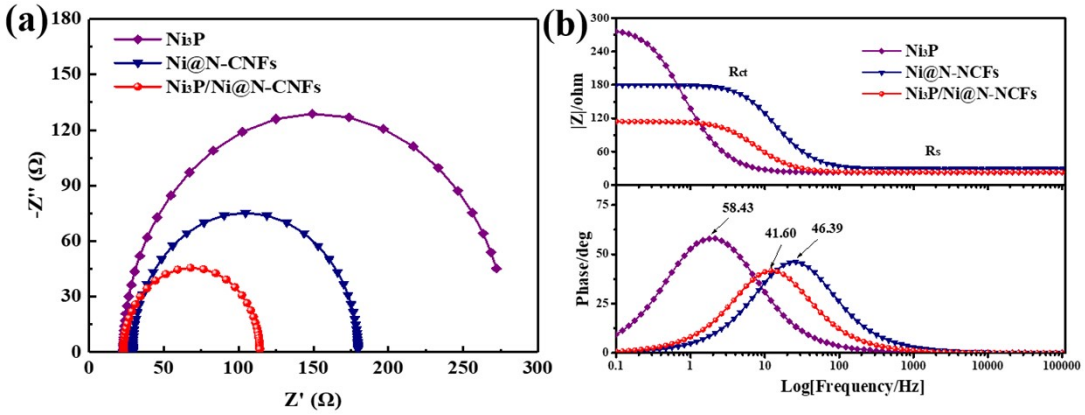

Fig. S26. (a) The double-layer capacitance (C_{dl}) for the evaluation of ECSA and (b) Bode plot of Ni_3P/Ni@N-CNFs, Ni@N-CNFs and Ni_3P in neutral media.

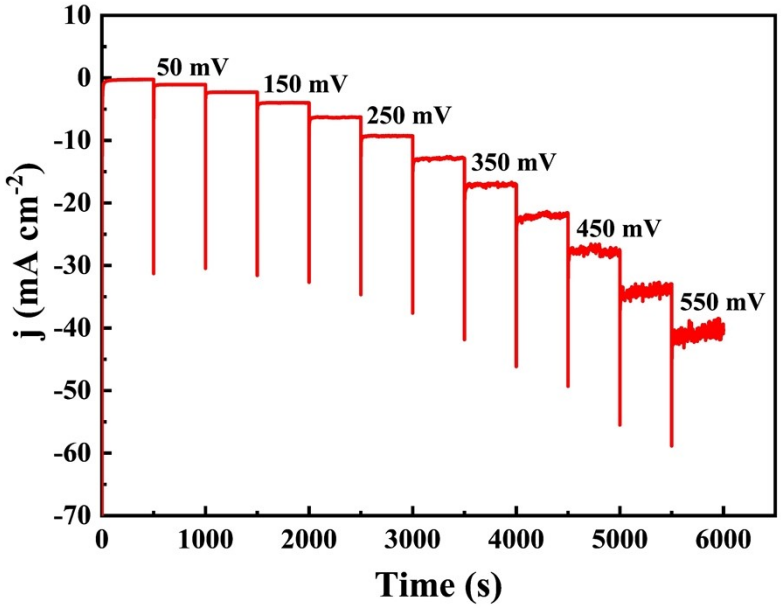

Fig. S27. Multi-step chronoamperometric curve at diverse overpotentials of Ni_3P/Ni@N-CNFs under neutral conditions.

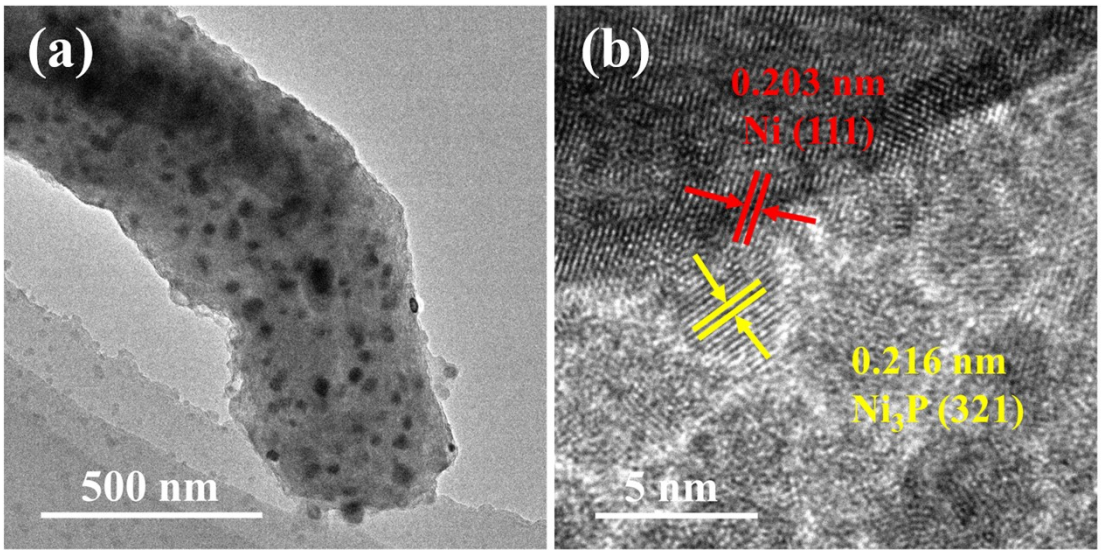

Fig. S28. (a) TEM image and (b) HRTEM image of the Ni_3P/Ni@N-CNFs after stability test of *i-t* curve for 60 h at pH 7.

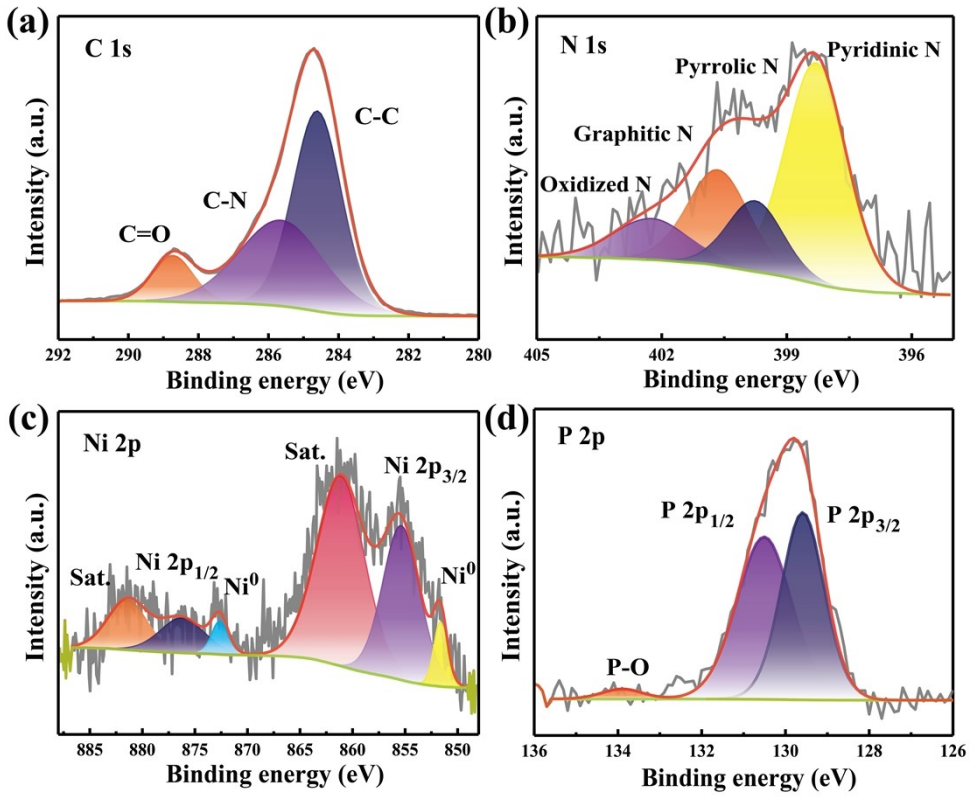

Fig. S29. XPS spectra of the Ni_3P/Ni@N-CNFs after HER electrochemical test in 1 M PBS: (a) C 1s; (b) N 1s; (c) Ni 2p; (d) P 2p.

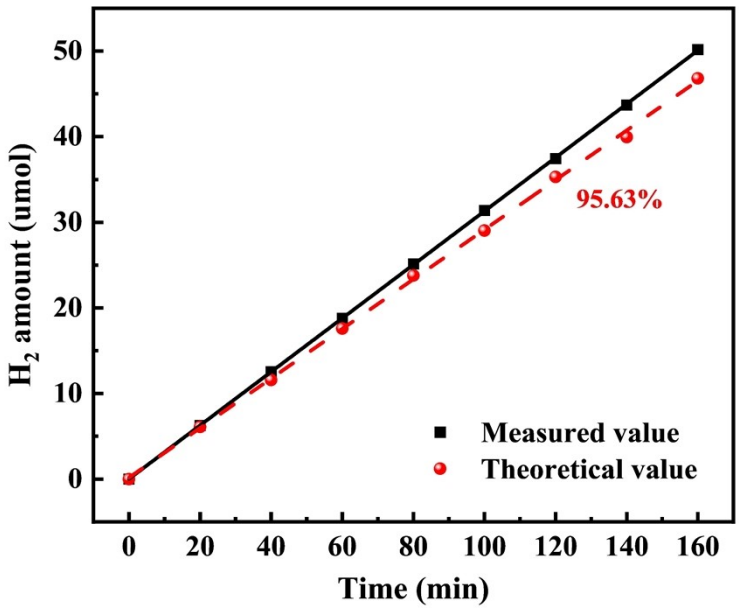

Fig. S30. Hydrogen production efficiency of Ni_3P/Ni@N-CNFs under neutral conditions.

Table S1. Surface elements contents of samples at different temperatures obtained by XPS.

Catalyst	C 1s [%]	N 1s [%]	Ni 2p [%]	P 2p [%]	O 1s [%]
Ni_3P/Ni@N-CNFs-600	57.93	6.29	11.48	1.58	22.72
Ni_3P/Ni@N-CNFs-700	60.77	7.97	7.98	1.36	21.92
Ni_3P/Ni@N-CNFs-800	51.90	3.77	15.36	1.09	27.87
Ni_3P/Ni@N-CNFs-900	60.71	2.14	5.10	0.71	31.34

Table S2. (a) The details for calculated fractions of each nitrogen species in the N 1s XPS spectrum.

Catalyst	Pyridinic N [%]	Pyrrolic N [%]	Graphitic N [%]	Oxidized N [%]
Ni_3P/Ni@N-CNFs-600	44.81	21.37	25.34	8.47
Ni_3P/Ni@N-CNFs-700	46.74	21.13	24.17	7.96
Ni_3P/Ni@N-CNFs-800	45.99	21.59	23.97	8.45
Ni_3P/Ni@N-CNFs-900	35.55	20.88	34.08	9.50

Table S2. (b) The details of the proportion of each N species in the whole sample were derived from the calculations.

Catalyst	Pyridinic N [%]	Pyrrolic N [%]	Graphitic N [%]	Oxidized N [%]
Ni_3P/Ni@N-CNFs-600	2.82	1.34	1.59	0.53
Ni_3P/Ni@N-CNFs-700	3.73	1.68	1.93	0.63
Ni_3P/Ni@N-CNFs-800	1.73	0.81	0.90	0.32
Ni_3P/Ni@N-CNFs-900	0.76	0.45	0.73	0.20

Table S3. Fitted data from Nyquist plots of as-prepared samples in electrocatalytic HER test under 0.5 M H_2SO_4.

Electrocatalysts	R_s (Ω)	R_{ct} (Ω)
Ni_3P/Ni@N-CNFs	6.48	24.84
Ni@N-CNFs	9.24	63.2
Ni_3P	4.55	221.7

Table S4. Comparison of HER performance between the results from the present research with other recently-reported metal phosphides in 0.5 M H_2SO_4.

	HER catalysts	Electrolyte	Overpotentials	Stability	References
1	Ni_3P/Ni@N-CNFs	0.5 M H_2SO_4	121 mV@10 mA cm^{-2}	60 h	*In this work*
2	MoP/MoNiP@NC	0.5 M H_2SO_4	137 mV@10 mA cm^{-2}	24 h	Chem. Eng. J. **2022**, 431, 133696.
3	Di-CoP/C	0.5 M H_2SO_4	136 mV@10 mA cm^{-2}	40000 s	J. Energy Chem. **2021**, 892, 115300.
4	Ni_2P-Co_2P/CC	0.5 M H_2SO_4	172 mV@10 mA cm^{-2}	50 h	Chem. Eng. J. **2021**, 424, 130444.
5	Ni-P/Ni/NF	0.5 M H_2SO_4	83 mV@10 mA cm^{-2}	40 h	Appl. Catal. B Environ. **2021**, 282 119609.
6	Ni_2P/Ni@C	0.5 M H_2SO_4	149 mV@10 mA cm^{-2}	1000 cycles	Adv. Funct. Mater. **2019**, 19015105.
7	CoP_3/CoMoP/NF HNAs	0.5 M H_2SO_4	125 mV@10 mA cm^{-2}	2 h	ACS Sustainable Chem. Eng. **2019**, 7, 9309-9317.
8	Co/Ni-doped MoP	0.5 M H_2SO_4	102 mV@10 mA cm^{-2}	10 h	Nano Energy **2020**, 70, 104445.
9	CoP-InNC@CNT	0.5 M H_2SO_4	153 mV@10 mA cm^{-2}	20 h	Adv. Sci. **2020**, 7, 1903195.
10	NiCoP-CNT@NiCo/CP	0.5 M H_2SO_4	82 mV@10 mA cm^{-2}	40 h	J. Mater. Chem. A **2021**, 9, 1150-1158.
11	Co-FeP NPs	0.5 M H_2SO_4	126 mV@10 mA cm^{-2}	60 h	Appl. Surf. Sci. **2020**, 510, 145427.
12	N-NiP_2	0.5 M H_2SO_4	153 mV@10 mA cm^{-2}	30 h	Sci. Adv. **2020**, 6 (1), eaaw8113.
13	Ni_2P-Fe_2P/NF	0.5 M H_2SO_4	128 mV@10 mA cm^{-2}	48 h	Adv. Funct. Mater. **2021**, 31, 2006484.
14	NiFeP/NCH	0.5 M H_2SO_4	216 mV@10 mA cm^{-2}	72 h	J. Am. Chem. Soc. **2019**, 141, 7906.
15	CoP NFs	0.5 M H_2SO_4	122 mV@10 mA cm^{-2}	30 h	ACS Catal. **2020**, 10, 412-419.
16	CoxP-NC-420	0.5 M H_2SO_4	125 mV@10 mA cm^{-2}	10 h	Electrochim. Acta **2022**, 403, 139643.

Table S5. Fitted data from Nyquist plots of as-prepared samples in electrocatalytic HER test under 1 M KOH.

Electrocatalysts	R_s (Ω)	R_{ct} (Ω)
Ni_3P/Ni@N-CNFs	3.1	27.50
Ni@N-CNFs	2.97	83.56
Ni_3P	1.45	227.90

Table S6. Fitted data from Nyquist plots of as-prepared samples in electrocatalytic HER test under 1 M PBS.

Electrocatalysts	R_s (Ω)	R_{ct} (Ω)
Ni_3P/Ni@N-CNFs	4.39	91.18
Ni@N-CNFs	4.05	150.6
Ni_3P	3.97	257.5

Table S7. Comparison of HER performance between the results from the present research with other recently-reported metal phosphides in 1 M KOH.

	HER catalysts	Electrolyte	Overpotentials	Stability	References
1	Ni_3P/Ni@N-CNFs	1 M KOH	145 mV@10 mA cm^{-2}	60 h	*In this work*
2	CoP-NC@NFP	1 M KOH	162 mV@10 mA cm^{-2}	50 h	Chem. Eng. J. **2022**, 428, 131115.
3	$FeCoP_2$@NPPC	1 M KOH	150 mV@10 mA cm^{-2}	12 h	ACS Appl. Mater. Interfaces **2021**, 13, 7, 8832-8843
4	CoP@FeCoP/NC YSMPs	1 M KOH	141 mV@10 mA cm^{-2}	20 h	Chem. Eng. J., **2021**, 403: 126312
5	MoP@NC	1 M KOH	149 mV@10 mA cm^{-2}	45 h	Appl. Catal., B **2020**, 263, 118358.
6	MoPS/NC	1 M KOH	158 mV@10 mA cm^{-2}	5 h	Appl. Catal., B **2019**, 245, 656-661
7	NiFeP@C	1 M KOH	160 mV@10 mA cm^{-2}	25 h	ACS Appl. Mater. Interfaces **2020**, 12 (17), 19447-19456.
8	Cr-doped FeNi-P/NCN	1 M KOH	190 mV@10 mA cm^{-2}	1000 cycles	Adv. Mater, **2019**, 31: 1900178
9	FeNiP/PG	1 M KOH	173 mV@10 mA cm^{-2}	10 h	J. Mater. Chem. A **2019**, 7, 14526.
10	Ni-CoP/Co_2P@NC	1 M KOH	117 mV@10 mA cm^{-2}	50 h	Chem. Eng. J. **2022**, 433, 133523.
11	Ni-P/Ni/NF	1 M KOH	129 mV@10 mA cm^{-2}	40 h	Appl. Catal., B **2021**, 282, 119609.
12	W_2C/WP@NC	1 M KOH	196.2 mV@10 mA cm^{-2}	12 h	ACS Appl. Mater. Interfaces **2021**, 13, 45, 53955-53964
13	CoP/Co_2P@NC	1 M KOH	198 mV@10 mA cm^{-2}	24 h	ACS Sustainable Chem. Eng. **2019**, 7, 8993-9001
14	FeP_2-NiP_2@PC	1 M KOH	248 mV@10 mA cm^{-2}	20 h	ACS Appl. Mater. Interfaces **2020**, 12, 727-733.
15	CoP-InNC@CNT	1 M KOH	125 mV@10 mA cm^{-2}	10 h	Adv. Sci. **2020**, 7, 1903195.
16	Mn-FeP	1 M KOH	173 mV@10 mA cm^{-2}	10 h	ACS Sustainable Chem. Eng. **2019**, 7, 14, 12419-12427

Table S8. Comparison of HER performance between the results from the present research with other recently-reported metal phosphides in 1 M PBS.

	HER catalysts	Electrolyte	Overpotentials	Stability	References
1	Ni_3P/Ni@N-CNFs	1 M PBS	187 mV@10 mA cm^{-2}	120 h	*In this work*
2	Cu_3P@NPC-CF	1 M PBS	192.52 mV@10 mA cm^{-2}	90 h	Sustain. Energy Fuels **2021**, 5, 2451-2457.
3	pFe/FeP	1 M PBS	250 mV@10 mA cm^{-2}	40 h	Chem. Eng. J., **2021**, 408, 127330.
4	CoP/Co_2P@NC	1 M PBS	459 mV@10 mA cm^{-2}	20 h	ACS Sustainable Chem. Eng. **2019**, 7, 8993-9001
5	0.02 Ni-MoP	1 M PBS	222 mV@10 mA cm^{-2}	1000 cycles	Nano Energy, **2020**, 70, 104445
6	MoP@NC NWs	1 M PBS	191 mV@10 mA cm^{-2}	5000 cycles	Appl. Catal. B Environ. **2020**, 263, 118358.
7	CoP/NiCoP/NC	1 M PBS	123 mV@10 mA cm^{-2}	80 h	Adv. Funct. Mater. **2019**, 29, 1807976.
8	Co_2P-NC-900	1 M PBS	315 mV@10 mA cm^{-2}	12 h	ChemSusChem. **2020**, 13, 351.
9	MoP700	1 M PBS	196 mV@10 mA cm^{-2}	2 h	ACS Catal. **2019**, 9, 8712-8718.
10	CoP-NC	1 M PBS	252 mV@10 mA cm^{-2}	10 h	Electrochim. Acta, **2021**, 375, 137966.
11	Ni_2P@NPCNFs	1 M PBS	185.3 mV@10 mA cm^{-2}	30 h	Angew. Chem. Int. Ed. **2018**, 57, 1963.
12	Ni_2P-Ru_2P/CCG-800	1 M PBS	113.38 mV@10 mA cm^{-2}	24 h	Chem. Eng. J. **2022**, 432, 134422.
13	CoP/PCNF	1 M PBS	191 mV@10 mA cm^{-2}	40000 s	Nano Res. **2018**, 11, 1274.
14	NiCo-P/Ni mesh	1 M PBS	250 mV@10 mA cm^{-2}	6 h	ACS Sustainable Chem Eng, **2019**, 7, 10734
15	Co-WP	1 M PBS	189 mV@10 mA cm^{-2}	60 h	Appl. Catal. B Environ. **2019**, 251, 162-167.
16	FeP/NCNSs	1 M PBS	409 mV@10 mA cm^{-2}	20 h	ACS Sustainable Chem.Eng. **2018**, 6, 11587
17	CoP@3D-NPC	1 M PBS	333 mV@10 mA cm^{-2}	6 h	Appl. Surf. Sci. **2019**, 476, 749.